Manufacturing Science and Education 2025

ACTA TECHNICA NAPOCENSIS

Series: Applied Mathematics, Mechanics, and Engineering
Vol. 68, Issue Special II, Month July, 2025

ANALYSIS OF THE IMPACT OF ROTATION SPEED ON THE FSW BEAD PROPERTIES FOR THREE OVERLAPPING ALUMINIUM ALLOYS

Ana GOGORICI, Daniela-Monica IORDACHE, Eduard-Laurențiu NIȚU, Claudiu BĂDULESCU

Abstract: *Friction Stir Welding (FSW) represents a cutting-edge and innovative welding method. It utilizes a non-consumable tool, avoids melting the material, operates in all positions, provides excellent mechanical properties, and has a minimal impact on the environment. This paper provides an analysis of the experimental results of friction stir welding beads for three different aluminum types alloys: AA7075, AA6061, and AA2024 welded together, overlapped. During the experiments, the position of the aluminum alloy plates and the advancing speed were kept constant, while the rotation speed was varied. The exit data recorded during the process and measured afterward on FSW beads will be analyzed and compared to determine the impact of rotation speed on the joint properties.*
Keywords: *FSW, AA2024, AA6061, AA7075, Roughness, Microhardness, Macrostructure.*

1. INTRODUCTION

The Friction Stir Welding process was invented and developed by The Welding Institute in the United Kingdom in 1991, specifically designed for welding similar aluminum alloy materials. The initial research was conducted on aluminum alloys, welding similar and dissimilar combinations. As a result, studies on the FSW process for aluminum alloys are abundant in both past and recent specialized literature, with numerous research studies analyzing the process and highlighting the benefits of this method in industrial applications [1]. The FSW process is characterized by the straightforward operation of a rotating tool, which possesses various configurations of active zones, being pressed against the surface of a minimum of two plates that are either overlapping or abutting each other. Then, the tool is inserted to approximately 85%-95% of the depth of the plates. In the next step, the tool moves along the weld bead to create the welding joint, and at the end of the welding bead, the tool is extracted from the joint [2], [3].

In recent years, more than 50% of FSW licenses and patents have been directed toward the following transportation industries: automotive, aeronautics, railway, aerospace, naval, and marine. The remaining percentage has been allocated to other sectors such as metal processing, electronics, machinery, research and development, equipment development, and others [4], [5]. The increasing use of FSW is due to its many benefits, such as good mechanical properties of the joints, tools that can be used for a long time, low environmental impact, and low production costs [4].

The flow of material in the area of the FSW weld bead can be influenced by several factors, such as: the design of the welding tool (shape and diameter of the pin, the shape and diameter of the shoulder, and others), the materials to be joined (mechanical and chemical properties, composition, thickness of the blank and others), the characteristics of the orientation and fixing device (its geometry, clamping force and others) and the working parameters (welding speed and rotation speed). Among these process characteristics, the most important are the process parameters that drive the generation of heat and the flow of material, which directly influence the properties and quality of the welded bead [6], [7].

The macrostructural analysis of the weld bead by the FSW process, for similarities and

differences alloys, has highlighted that it is divided into zones: Weld Zone (WZ), Thermo-Mechanically Affected Zone (TMAZ), Heat-Affected Zone (HAZ) and Base Material (BM). Studies indicate that the configuration and dimensions of the macrostructural zones are contingent upon the shape and size of the tool [4].

Recent studies have focused on microstructure evolution in FSW joints for different aluminum alloys. In the case of AA7075 and AA5083 beads, it was found that the substantial differences in the base materials' properties had a strong impact on grain recrystallization in the weld zone [8]. The analysis of the FSW weld joint between the AA6060 alloy (retreating side) and the AA7003 alloy (advancing side), both 4,5 mm thick, showed that the weld core comprises fine grains with an average size of 11,1 μm. These grains contain the AA7003 alloy from the advancing side [9]. The analysis of the microstructure of FSW joints is challenging because the materials in the weld zone undergo plastic deformation and dynamic recrystallization. It was observed that the grains become finer as they get closer to the weld bead core.

Studies on FSW beads of different materials show that the advancing speed affects weld microhardness and strength. A moderate increase improves mechanical properties, but excessive speeds cause non-homogeneous structures, weakening the joint. [10]

Guido and colleagues highlight the influence of rotational speed on heat input and the microstructure of the FSW joint for different aluminum alloys. A lower speed ensures an optimal balance, promoting efficient plasticization without overheating. This leads to a uniform microstructure and consistent hardness, which are essential for the joint's mechanical integrity. In contrast, higher speeds cause variations in microstructure and hardness, affecting the weld performance [11].

The visual appearance of the FSW weld bead on the upper surface consists of semicircular traces, and the surface opposite the tool contact area shows no obvious changes. The process parameters influence the texture of the FSW weld bead. For FSW weld beads made between different aluminum alloys, it has been found that a low speed value leads to the appearance of pores, increased roughness, and penetration of the material by the shoulder of the active element, and a high-speed value also generates pores [12].

This paper aims to analyze the effect of rotational speed variation on the characteristics of the FSW weld bead for three different aluminum alloys positioned in an overlapping configuration. The aluminum alloys AA2024, AA6061, and AA7075 were welded simultaneously to evaluate their microhardness, roughness, macrostructure, and microstructure behavior under these conditions.

This paper investigates the influence of rotational speed on friction stir weld bead (FSW) characteristics in an overlapping configuration of three different aluminum alloys: AA2024, AA6061, and AA7075. These three aluminum alloys are recognized and widely used in aviation due to their excellent mechanical strength properties, high strength-to-weight ratio, and good corrosion performance.

The study explores the behavior of these three different alloys when welded simultaneously, focusing on the following aspects: temperature and vertical force evolution, macrostructure analysis, microhardness analysis, and roughness evolution analysis.

This study provides insight into the mechanical and structural behavior of the weld bead made by FSW in the case of an overlapping weld between three different aluminum alloys, widely used in the aeronautical industry. It highlights the impact of rotational speed on the final properties of the weld bead.

2. EXPERIMENTAL PROCEDURE

This experimental study used three specific aluminum alloys: AA2024, AA6061, and AA7075. The plates were welded together in an overlapping arrangement.

The dimensions of the plates for these materials are 2 mm thick, 140 mm wide, and 250 mm long. Tables 1 and 2 display the effective mechanical properties and chemical composition of all three materials.

According to Figure 1, the three distinct materials were initially arranged in the following sequence: AA2024 at the top, AA6061 in the intermediate position, and AA7075 at the bottom. After that, they were welded together.

Table 1

Chemical composition pertaining to aluminum alloys AA2024, AA6061, and AA7075 (in percent by weight)

	AA2024	AA6061	AA7075
Si	0,10	0,74	0,05
Fe	0,11	0,40	0,10
Cu	4,40	0,22	1,60
Mn	0,47	0,14	0,05
Mg	1,50	0,90	2,70
Cr	0,01	0,18	0,19
Zn	0,14	0,09	5,80
Ti	0,04	0,05	0,05
Ti+Zr	0,05	-	0,01

Table 2

Mechanical properties pertaining to aluminum alloys AA2024, AA6061, and AA7075

	AA2024	AA6061	AA7075
UTS (MPa)	464 - 466	317 - 319	593 - 594
YS (MPa)	344 – 348,8	286 -290	531 - 532
Elongation(%)	17-18	10 – 12	11 - 12

In Friction Stir Welding, input parameters include the tool's rotation speed in revolutions per minute (rpm) and welding speed in millimeters per minute (mm/min). In the experiments, the welding speed remained constant across trials, while the tool's rotation speed was set to two levels (minimum and maximum), as shown in Table 3.

Table 3

Experimental plan for FSW process

Experiments code	1.1	1.2
Advancing speed – w mm/min	70	
Rotation speed - n rpm	600	1400

The welding process was conducted in three distinct phases: firstly, the tool was vertically inserted through the upper plate, the second plate, and partially into the third plate; secondly, the tool traversed along the welding bead, effectively joining the plates; finally, the tool was vertically retracted. This procedure results in a hole in the materials, the diameter of which is equivalent to that of the pin tool.

The cylindrical welding tool for aluminum alloys has a shoulder diameter of 22 mm and a height of 5.3 mm for the threaded M6 pin. It is made of P20+S (sintered tungsten carbide), as shown in Figure 2.

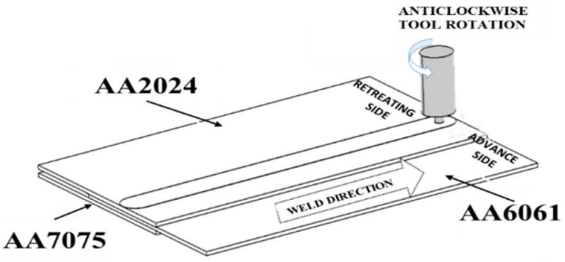

Fig. 1. FSW – position of materials

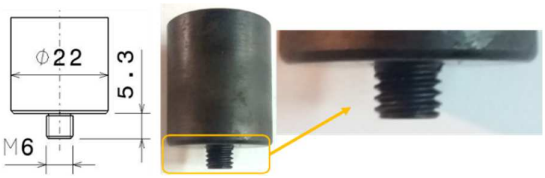

Fig. 2. Welding tool

Two output parameters were measured during the FSW process: temperature and vertical force. A FLIR A40M thermographic infrared camera, which measures temperatures from -40 to +2000 degrees Celsius, was used. Therma CAMTM Researcher software extracted measurement data along the welding line near the tool shoulder.

The vertical force was quantified employing a mechanical apparatus integrated with a fixed force transducer, designated as model AM, exhibiting a measurement range from 0 kN to 20 kN, affixed to the primary spindle of the Friction Stir Welding machine. This vertical force is paramount for attaining effective welding and signifies the intensity with which the tool penetrates the base material.

After the welding process, the samples were measured for roughness and microhardness. The roughness was assessed utilizing an electronic roughness tester, model MarSurf PS 10, whereas the microhardness was evaluated using an electronic microhardness tester, model Innova Test Falcon 500.

3. RESULTS AND DISCUSSIONS

3.1 Temperature evolution analysis

Figure 3 illustrates the temperature changes during the FSW process along the weld bead length for both experimental conditions.

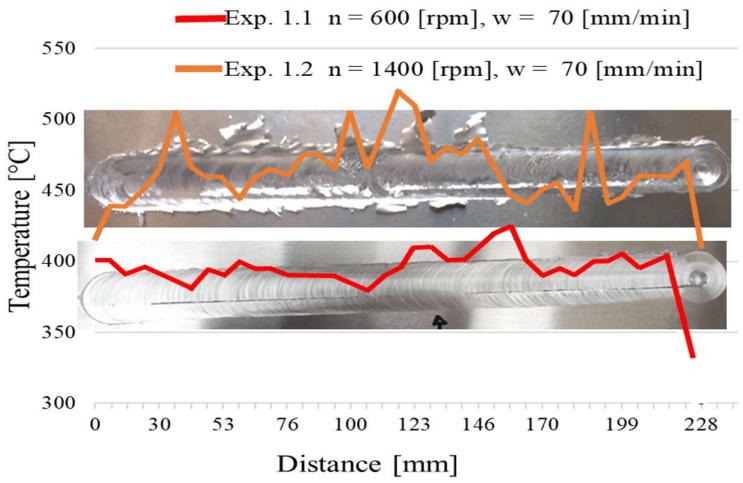

Fig.3. Temperature evolution

The red line represents the experiment with code 1.1, and the orange line represents experiment 1.2, an experiment for which the rotation speed parameter increased by 130% compared to the first. Behind the graphs are represented the two FSW weld beads; the position of the graphs on the length of the weld beads corresponds to the situation recorded during the performance of the experiments. The melting temperature of the material positioned in the upper part of the weld bead, the part from which the thermographic infrared camera captured the information, is 500 °C for aluminum alloy AA2024.

According to Table 4, which shows the temperature value recorded at specific points of the weld bead and according to the graph presented in Fig.3, throughout conducting of the two experiments in the experimental plan, respectively, along the entire length of the FSW weld bead, the temperature values recorded for experiment .1.2 were higher by approximately 60-70 °C, representing a difference of approximately 6-7 %.

Table 4

The temperature value recorded at different points of the weld bead °C

Experiments code	Distance from the start of the weld bead mm			
	10	80	150	220
1.1	400	390	410	400
1.2	440	460	485	460

The maximum temperature recorded during the process was 520 °C for experiment 1.2. This temperature was recorded at 120 mm from the start of the weld bead. For experiment 1.1. the maximum temperature reached during the process was 425 °C and was recorded at 160 mm from the start of the weld bead.

With the increase in the rotation speed of the tool, there is an increase in the temperature recorded on the weld bead during the FSW process. This phenomenon can be explained by the fact that at higher rotational speeds, there is increased friction between the tool and the material to be processed, leading to increased temperatures in the joint area. Also, the visual appearance of the weld bead made with the higher rotation speed and, as well higher temperature, is less uniform and has a surplus of burrs.

3.2 Vertical force evolution analysis

Figure 4 shows both cases' vertical force evolution along the weld bead length during the FSW process.

Throughout the FSW welding process and along the entire length of the weld bead, the maximum vertical force recorded was consistent for the experiment with code 1.1, and the minimum value corresponded to maximum rotation speed. It was found that, as anticipated due to the impact of temperature on the malleability of the joined materials, the recorded values for vertical force are inversely proportional to the temperatures observed. Therefore, the higher the temperature that the welding tool generates during the FSW process, the lower the vertical force.

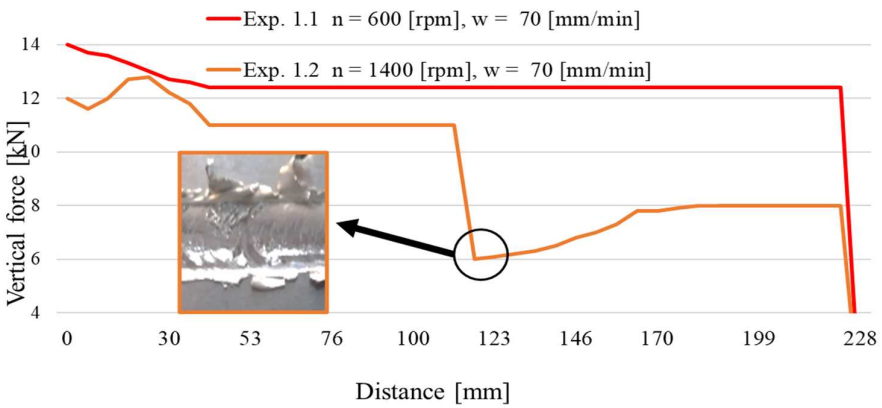

Fig.4. Vertical force evolution

In both experiments, the vertical force measured in the first 40 mm from the start of the weld bead is higher. This interval indicates the area where the process is stabilizing. After the process stabilizes, for experiment noted with 1.1, the vertical force remains constant throughout the weld bead at a value of 12.4 kN. In experiment 1.2, where the recorded temperature during the process was higher, the vertical force was constant at a value of 11 kN along the length of the weld bead in the range of 40-120 mm.

At 120 mm from the beginning of the weld bead, at the same time as the maximum recorded temperature value, the vertical force suddenly decreases to the value of 6 kN due to excessive heating of the sample, after which it grows slightly and stabilizes at the value of 8 kN for the rest of the weld bead. The visual appearance of the weld bead in the area of sudden variation differs from the rest, presenting irregularities and the appearance of prominent 'onion leaves'.

The influence of the rotation speed parameter variation on the two characteristics recorded during the realization of the FSW weld bead and the direct influence of temperature on the vertical force recorded during the FSW welding process is observed.

3.3 Analysis of macrostructure evolution

The evolution of the macrostructure was recorded at two positions on the welding beads, specifically at 140 mm and 230 mm from the start of the weld. For the experiment with code 1.1, microstructures are represented in Fig.5 and Fig.6. For the experiment with code 1.2, microstructures are represented in Fig.7 and Fig.8. The advance side and the retract part of the material by tools are highlighted in all four figures with the letters A—advance side and R—retract side.

Analysis of the macrostructures related to the two experiments conducted revealed the presence of four specific areas in an FSW joint: the weld nugget at the center of the joint, which has the highest degree of plastic deformation; the thermo-mechanically affected area close to the core; and the thermally affected area where changes in the properties of the base material result solely from the temperatures to which it is subjected and the area of the base material.

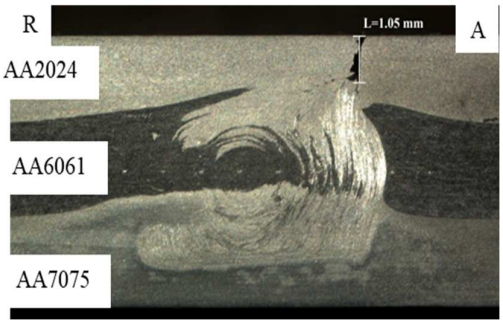

Fig.5. Macrostructure for exp 1.1 at 140 mm

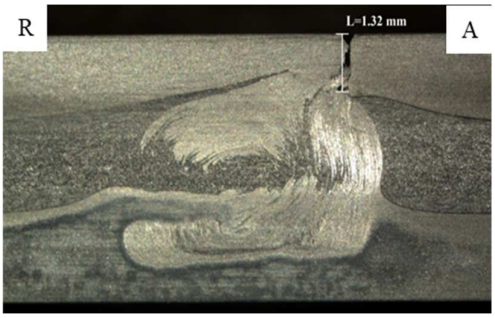

Fig.6. Macrostructure for exp 1.1 at 230 mm

The weld nugget of the FSW weld bead is improved for the experiment performed with a higher rotational speed value (n=1400 rpm), Fig.7 and Fig.8; the combination of all three materials is easily noticeable, especially when compared to the experiment conducted with the lower value of this parameter. (n=600 rpm), Fig.5 and Fig.6. Defects are also present in the two weld beads analyzed. Experiment 1.1 shows a single crack-type defect detected in the upper material along the entire length of the weld bead, and experiment 1.2 presents defects types: lack of fusion, tunnels, and pores. The position of defects is approximately similar for both experiments, mainly on the advancing side of the weld bead.

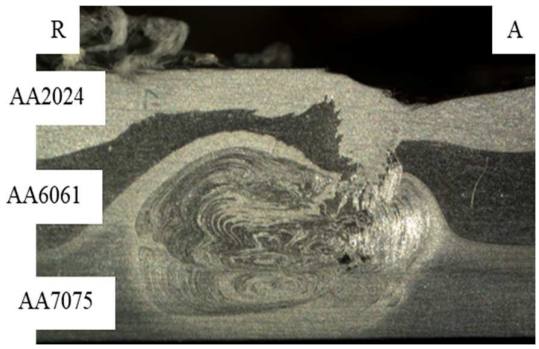

Fig.7. Macrostructure for experiment 1.2 at 140 mm.

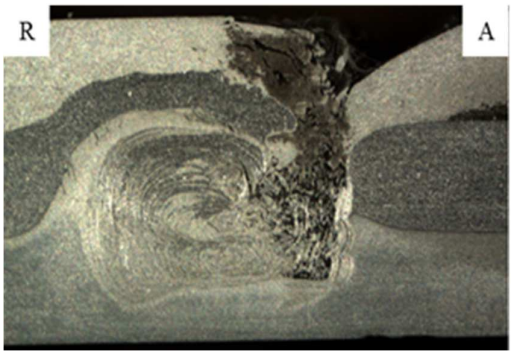

Fig.8. Macrostructure for Experiment 1.2 at 230 mm.

3.4 Microhardness evolution analysis

This study measured micro-hardness at the same position on welding beads, 140 mm from the start weld. Measurements were taken perpendicular to the tool movement direction at three depths: 1 mm, 3 mm, and 5 mm from the weld surface for each aluminum alloy. The two graphs also represented the microhardness of the aluminum alloys before joining: AA2024 – 141,3 HV0.3, AA6061 – 41,1 HV0.3, and AA7075 – 188,8 HV0.3. The missing values in the two graphs, Fig.9 and Fig.10, represent defects and pores in the weld bead.

According to the macrostructure, comparing the two microhardness graphs shows a better mixing of the aluminum alloys and a greater distribution of the values recorded for microhardness when the rotational speed used had the maximum value, respectively, in experiment 1.2, Fig.10.

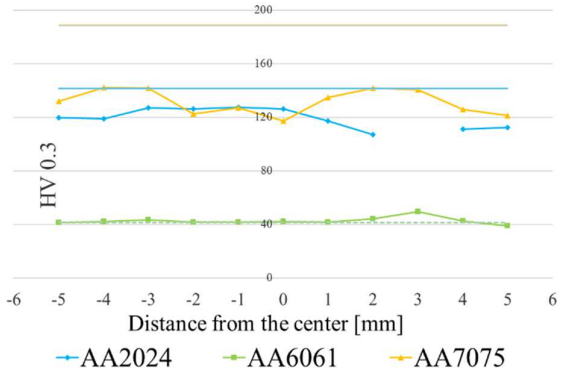

Fig.9. Microhardness evolution for exp 1.1 at 140 mm

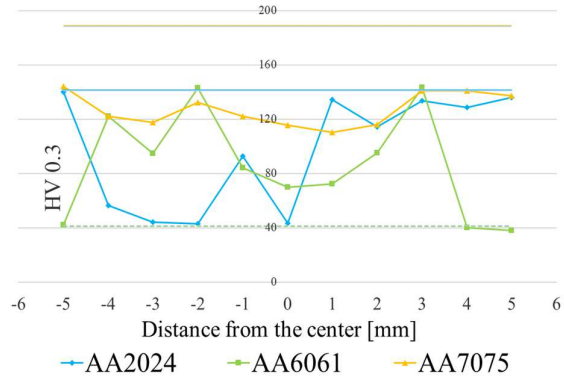

Fig.10. Microhardness evolution for exp.1.2 at 140 mm

3.5 Roughness evolution analysis

The visual aspects of the two weld beads are shown in Fig.11 and Fig.12. Experiment 1.1 shows a crack along the entire length of the weld bead, on the advance side of the tool, and experiment 1.2 shows excessive burrs, the causes of which may be high temperatures during the welding process. Burrs are considered minor defects and can be easily removed.

The roughness of the welded s was determined in three areas specific to each weld bead made: 90 mm, 110 mm, and 200 mm from the start of the weld bead. The measured values are presented in Table 5.

Table 5

The roughness value measured at different points of the weld bead μm			
Experiments code	Distance from the start of the weld bead mm		
	90	110	200
1.1	2,6	1,7	2,2
1.2	1.4	1.0	2.1

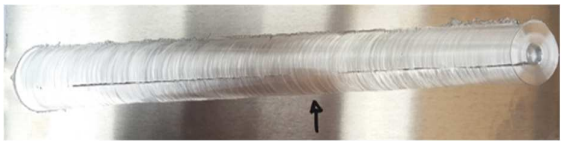

Fig.11. Visual aspects of exp.1.1

Fig.12. Visual aspects of exp.1.2

Regarding roughness, both experiments recorded a stable evolution along the weld beads. The increase in the rotational speed value leads to a slight decrease in roughness on all three analyzed areas.

4. CONCLUSION

This study examines the effect of rotation speed on the characteristics of Friction Stir Welding beads made from three aluminum alloys, AA7075, AA6061, and AA2024 positioned overlapping. The results highlight the significant impact of tool rotation speed on weld bead properties.

The rotational speed of the tool directly affects the temperature achieved during the process: as the tool's rotational speed increases, so does the temperature. Another significant factor influencing the temperature reached is the aluminum alloy located in the upper part of the joint. For both experiments, the AA2024 alloy was placed in the upper section.

The vertical forces observed during the process are directly affected by the temperature achieved, such that an increase in rotational speed results in a decrease in axial forces.

The macrostructure of the welded joint demonstrates that an increased rotational speed enhances the mixing and homogenization of the three materials; however, the parameters employed did not preclude the emergence of defects within the weld bead.

The outcomes of the microhardness analysis, akin to the macrostructure, indicated that applying an elevated rotation speed resulted in enhanced homogenization of the aluminum alloys and a more equitable distribution of microhardness values.

The roughness was quantified in three distinct areas. It was observed that increased rotational speed results in a marginal reduction in roughness throughout the entirety of the weld bead. The weld bead created at the higher rotational speed consistently showed burrs along its entire length.

Friction stir welding for a range of three different aluminum alloys is a challenge, given the significant differences between the physical and chemical properties of the alloys to be joined. In this context, future research will focus on the following essential directions: the analysis and definition of the parameters that can lead to the realization of defect-free weld seams and the study of the applicability of FSW welded joints for three different aluminum alloys to the realization of components in the aeronautical industry.

FSW can become a leading solution in various industrial fields by exploring different input parameters, alloys with varied characteristics, and special configurations during the process.

The project was conducted with the assistance of the National R&D Institute for Welding and Material Testing, ISIM Timișoara.

5. REFERENCES

[1] Magalhaes, V.M., Leitao C., Rodrigues D.M., *Friction stir welding industrialisation and research status*, SAGE Publications, Sci Technol Weld Joi Vol.23, No.5, 400-409, 2018.

[2] Mostafa, A., Tarasankar D., Parviz A., Tomasz S., *Recent advances in friction stir welding/processing tools,* Journal of Manufacturing Processes 142, 99-156, 2025.

[3] Kalemba-Rec, I., Kopyscianski M., Miara D., Krasnowski K., *Effect of process parameters on mechanical properties of friction stir welded dissimilar 7075-T651 and 5083-H111 aluminum alloys*, Int. J. Adv. Manuf. Technol., Vol. 97, pp. 2767–2779, 2018.

[4] Shalok, B., Sudhir K.D., Indejeet S., Dinesh K., Swapnil S.B., Mohamed R.A., Seyed R.K., *A Review of Recent Developments in Friction Stir Welding for Various Industrial Applications*, Journal of Marine Science and Engineering, 12(1):71, 2023

[5] Bosneag, A., Constantin M.A., Nitu E., Iordache M., *Friction Stir Welding of three dissimilar aluminium alloy used in aeronautics industry*, IOP Conference Series - Materials Science and Engineering, Vol. 252, 012041, DOI: 10.1088/1757-899X/252/ 1/012041, 2017.

[6] Noah, E. E., Stephen A., Wai L.W., Vivek P., Rasheedad M.,*Taguchi-based optimisation of FSW parameters for advancement in aerospace materials: Al-Li 2060 alloy,* Heliyon 10, e41048, 2024.

[7] Yuanpeng, L., Kun C., Guang Z., Zhenghe W., Shuai T., Kaishan N., *Numerical calculation and analysis of FSW process for high strength 7075 aluminum alloy based on cel method,* U.P.B. Sci. Bull., Series D, Vol.86, Iss.1, ISSN 1454-2358, 2024.

[8] Ahmed, M., Ataya S., El-Sayed S.M., Ammar H., Ahmed E., *Friction stir welding of similar and dissimilar AA7075 and AA5083*, Journal of Materials Processing Technology, Vol. 242, pp. 77-91, 2017.

[9] Dong, J., Zhang D., Zhang W., Zhang W., Qiu C., *Microstructure Evolution during Dissimilar Friction Stir Welding of AA7003-T4 and AA6060-T4*, Materials, 11, 342, 2018.

[10] Bipin, K. S., Sujeet K. G., Anshu A., Ritesh K. S., Sanjiv K. T., Amir R. S., Rajat U., *Parametric study to investigate mechanical properties of welded dissimilar Al6063 and Al 7073 alloys through FSW process,* Eng. Res. Express 6, 035406, doi.org/10.1088/ 2631-8695/ad5f79, 2024.

[11] Guido, D. B., Chiara B., Mohamed C., Davide C., Gianluca B., *Effect of Rotational Speed on Mechanical Properties of AA5083/ AA6082 Friction Stir Welded T-Joints for Naval Applications*, Metals, 14, 1410, doi.org/10.3390/met14121410, 2024.

[12] Cioffi, F., Ibáñez J., Fernández R., González-Doncel G., *The effect of lateral off-set on the tensile strength and fracture of dissimilar friction stir welds, 2024Al alloy and 17%SiC/2124Al composite*, Materials and Design, Vol. 65, pp. 438–446, 2013.

ANALIZA IMPACTULUI VITEZEI DE ROTAȚIE ASUPRA PROPRIETĂȚILOR ÎMBINĂRII FSW PENTRU TREI ALIAJE DE ALUMINIU SUPRAPUSE

Procedeul de sudarea prin frecare cu element active rotator, denumit pe scurt FSW, este o tehnică de sudare avansată și inovatoare. Folosește o sculă rotativă neconsumabilă, evită topirea materialului, nu are restricții cu privier la poziția cordonului de sudură, îmbinarea prezintă proprietăți mecanice bune și are un impact redus asupra mediului. Această lucrare prezintă rezultatele experimentale ale îmbinărilor realizate utilizând procedeul de sudare prin frecarecu element active rotitor pentru trei aliaje de aluminiu diferite: AA2024, AA6061 și AA7075 sudate suprapus. Pentru realizarea experimentelor s-a păstrat poziția plăcilor și viteza de avansare a scule, iar viteza de rotație a scului a fost variată. Datele de ieșire înregistrate în timpul procesului și măsurate ulterior pe cordonul de sudură vor fi analizate și comparate pentru a defini impactul vitezei de rotație asupra proprietăților îmbinării.

Ana GOGORICI, Lecturer, National University of Science and Technology POLITEHNICA Bucharest, Pitesti University Center, Manufacturing and Industrial Management Department, *ana.bosneag@upb.ro*, Targul din Vale Street, no. 1, Pitesti, Arges, Romania, +40723297070.

Daniela Monica IORDACHE, University habilitated professor, National University of Science and Technology POLITEHNICA Bucharest, Pitesti University Center, Manufacturing and Industrial Management Department, *daniela.c.iordache@upb.ro*, Targul din Vale Street, no. 1, Pitesti, Arges, Romania, 0348 453 160.

Eduard Laurențiu NIȚU, University habilitated professor, National University of Science and Technology POLITEHNICA Bucharest, Pitesti University Center, Manufacturing and Industrial Management Department, *eduard.l.nitu@upb.ro*, Targul din Vale Street, no. 1, Pitesti, Arges, Romania, 0348 453 159.

Claudiu BĂDULESCU, University habilitated associate professor - Researcher, UBS – UBO - ENSTA Bretagne - ENIB, UMR CNRS 6027, Research Institute Dupuy de Lôme (IRDL), *claudiu.badulescu@ensta-bretagne.fr*, François Verny Street, no. 2, 29806 Brest Cedex 9, France.